Adaptive underwater image recovery using polarimetric imaging

Liang, Zheng, Zhao, Congcong , Wang, Yafei, Ding, Xueyan, Mi, Zetian, et al.

Zheng Liang, Congcong Zhao, Yafei Wang, Xueyan Ding, Zetian Mi, Xianping Fu, "Adaptive underwater image recovery using polarimetric imaging ," Proc. SPIE 11069, Tenth International Conference on Graphics and Image Processing (ICGIP 2018), 110692L (6 May 2019); doi: 10.1117/12.2524394

SPIE.

Event: Tenth International Conference on Graphic and Image Processing (ICGIP 2018), 2018, Chengdu, China

Adaptive Underwater Image Recovery Using Polarimetric Imaging

Zheng Liang, Congcong Zhao, Yafei Wang, Xueyan Ding, Zetian Mi, Xianping Fu*
Information Science and Technology College, Dalian Maritime University, Dalian 116026, China
fxp@dlmu.edu.cn

ABSTRACT

Underwater image generally suffers from color degradation and poor visibility due to the attenuation and scattering of the propagated light. To restore the real environment of the underwater, most of previous methods only consider the scattering in the polarimetric image recovery model. To compensate for the absorption in different wavelengths, a simple but effective underwater image enhancement method that based on the adaptive polarimetric image recovery model is proposed in this paper. In order to achieve automatic estimation of model parameters, the backscattered light estimation is based on the quad-tree decomposition to extract the fully backscattered area automatically. The experimental results demonstrate that the visual quality of underwater images are efficiently enhanced.

Keywords: underwater image, adaptive image recovery model, polarimetric imaging, backscattered light.

1. INTRODUCTION

Underwater optical imaging has been applied in different fields of underwater science research and industrial production [1], such as underwater robot [2], underwater pipeline detection technology [3] and provided samples for marine biology [4]. However, underwater image captured by cameras often suffers from color shift and contrast degradation due to the scattering and absorption by the suspend particles existing in water. Several methods are proposed to improve the quality of underwater images, which can be divided into two categories, one is based on the single hazy image. Such as, Histogram Equalization (HE) [5] is a traditional and effective method for underwater degraded image enhancement, but the interested details may not reach the level we want. Dark channel prior is proposed by He et al. to restore the hazy image, but it is succesfully applied to the restoration of underwater image based on the similarity between hazy images and underwater images. Li et al. [6] ultilized minimum information loss and histogram distribution prior to enhance underwater images. The other is based on the multiple hazy images. For example, Schechner et al. [7, 8] was the first to propose polarimetric recovery method based on the polarization characteristics of backscattered light, they conducted their experiments using two images captured at orthogonal polarization states, achieving better visual quality in turbid medium. Inspired by Schechner's method, various improved methods have been proposed [9-13]. For example, an effective polarimetric dehazing method is proposed based on the angle of polarization by Liang et al. [11, 13], this method needs four images captured at four different polarization, therefore, the complexity of the system would increase.

There is a great difference between underwater imaging conditions and land-based imaging conditions. Scattering is the main cause of image quality degradation acquired by land-based imaging. But the main cause is the scattering and absorption in water, when the natural illumination enters the water, it has a strong color-dependent attenuation, which typically becomes predominantly green-blue [8]. As shown in Fig. 1, there are two sources that we sense when imaging underwater. The first source is the scene object at distance d, whose radiance will attenuate because of the absorption and scattering in the water and even gets blurred. The image corresponding to this degraded source is the signal light, (accounting for both the direct transmission and the forward scattering). In the process of transmitting to the camera, the object radiance is partially lost due to the absorption and scattering, and the fraction that finally reaches the camera is called direct transmission. The forward scattering component is similar to the direct transmission. However, it represents light scattered forward at small angles relative to LOS. The second source is the ambient illumination. Part of light is scattered to the camera under the influence of the particles in the water, which is called the backscattered light. As the distance d between the camera and the object increases, the backscattered light A becomes more apparent, and the signal light D emitted from the object is gradually weakened due to the influence of absorption and scattering.

Tenth International Conference on Graphics and Image Processing (ICGIP 2018), edited by
Chunming Li, Hui Yu, Zhigeng Pan, Yifei Pu, Proc. of SPIE Vol. 11069, 110692L
© 2019 SPIE · CCC code: 0277-786X/19/$18 · doi: 10.1117/12.2524394

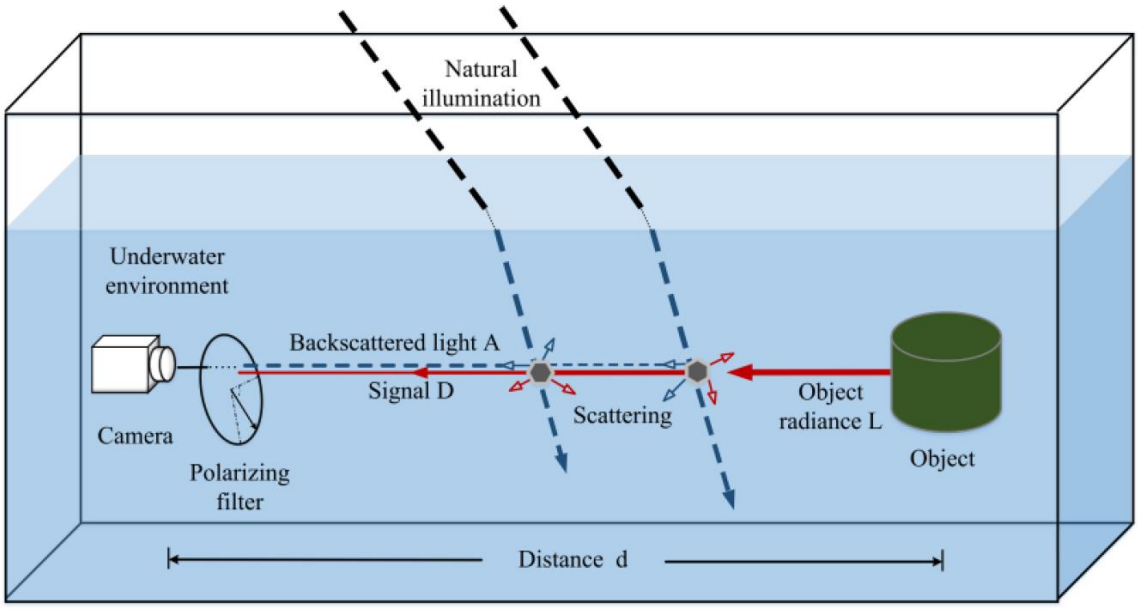

Figure 1. Underwater imaging through a polarizer (analyzer) in our experiment.

In fact, there have some problems with the most of the methods mentioned, they applied the atmosphere polarimetric image dehazing model directly to the restoration of underwater degraded images without considering the particularity of underwater environment [8, 14]. In addition, when estimating parameters of the model, the author often manually selects a small area "at infinity" to estimate [8, 14]. The small area is termed fully backscattered area in this paper, because the small area "at infinity" is not affected by light absorption. To solve these problems mentioned above, (1) an adaptive underwater polarimetric image dehazing model for underwater environment is applied; (2) extracting the fully backscattered area automatically by using the quad-tree decomposition to estimate parameters of the novel model is proposed.

2. PROPOSED METHODOLOGY

2.1 Adaptive Underwater Imaging Recovery Model

In the optical imaging system, light received by the camera mainly includes two components, one is the signal light of the scene object, and the other is backscattered light. The total intensity image can be expressed mathematically as:

$$I(x,y) = L(x,y)t(x,y) + A_\infty(1-t(x,y)) \tag{1}$$

where (x,y) is the pixel coordinate, $I(x,y)$ is the image acquired by the camera, $L(x,y)$ is the object radiance without scattering and absorption, A_∞ is the backscattered light which extends to infinity. Note that $t(x,y) = e^{-\beta d(x,y)}$ denotes the transmission from object to camera, where β is the attenuation coefficient of the medium, $d(x,y)$ is the distance between the camera and the object. The term $D(x,y) = L(x,y)t(x,y)$ is the signal light of the scene object that reached to the camera, and the term $A(x,y) = A_\infty\left(1-t(x,y)\right)$ is the backscattered light. $L(x,y)$ can be derived as:

$$L(x,y) = \frac{I(x,y) - A(x,y)}{1 - A(x,y)/A_\infty} \tag{2}$$

In the water, by exploring the differences in light attenuation between in atmosphere and in water, an adaptive underwater polarimetric image dehazing model is proposed:

$$L(x,y)=\frac{I(x,y)-A(x,y)}{k(1-A(x,y)/A_{\infty})} \tag{3}$$

where k is compensation vector for absorption.

Generally speaking, there are two key parameters involve in the polarimetric methods: the backscattered light $A(x,y)$ and the backscattered light which extends to infinity A_{∞}. Although there are several automatic methods of estimating $A(x,y)$ and A_{∞} have been reported in single haze removal techniques, the estimation of $A(x,y)$ and A_{∞} could not be realized automatically during the process of polarimetric dehazing imaging. In order to achieve the real time and applicability of the proposed method, with the inspiration of the quad-tree decomposition technique [15], $A(x,y)$ and A_{∞} can be estimated automatically, which is particularly important for the case of the underwater real-time polarimetric dehazing applications. Fig. 2 shows the flowchart of the proposed method.

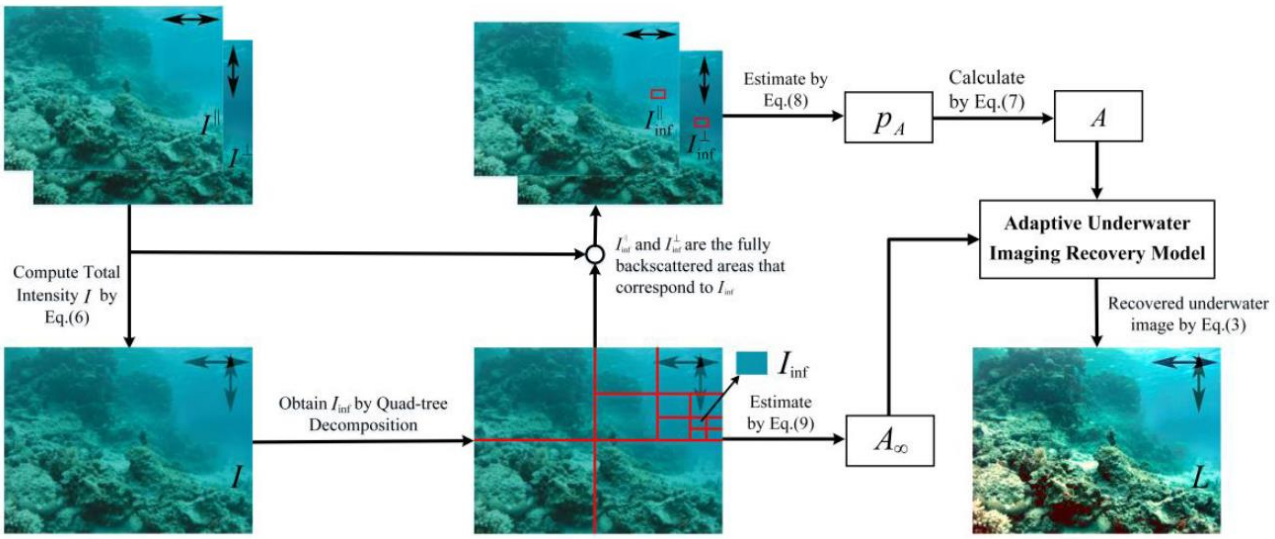

Figure 2. Flowchart of the proposed method.

2.2 Estimation of Model Parameters

In the underwater polarimetric dehazing method, two orthogonal polarimetric images are captured by rotating the analyzer to the parallel and orthogonal polarization state, $I^{\parallel}(x,y)$ and $I^{\perp}(x,y)$. $I^{\parallel}(x,y)$ is called the "worst state" image with the most backscattered light $A^{\parallel}(x,y)$

$$I^{\parallel}(x,y)=\frac{D(x,y)}{2}+A^{\parallel}(x,y) \tag{4}$$

and $I^{\perp}(x,y)$ corresponds to the "best state" image with the least backscattered light $A^{\perp}(x,y)$

$$I^{\perp}(x,y)=\frac{D(x,y)}{2}+A^{\perp}(x,y) \tag{5}$$

In addition, the total intensity image is calculated by:

$$I(x,y)=I^{\parallel}(x,y)+I^{\perp}(x,y) \tag{6}$$

Because of the partial polarization of the backscattered light, the degree of polarization (DOP) of the backscattered light A is given by $p_A = (A^{\parallel} - A^{\perp})/(A^{\parallel} + A^{\perp})$. Therefore, According to Eqs. (4, 5), the backscattered light radiance A can be estimated by:

$$A(x,y) = \frac{I^{\parallel}(x,y) - I^{\perp}(x,y)}{p_A} \tag{7}$$

According to Eqs.(3,6,7), only A_∞ and p_A are acquired to obtain the object radiance $L(x,y)$, In order to estimate p_A, Schechner et al. [8] manually selected a small area "at infinity" in these two polarization images. In this paper, quad-tree decomposition method is used to find the area automatically. According to the variance of pixel values is generally low of the fully backscattered area, We first obtain the total intensity image $I(x,y)$, and divide it into four rectangular regions. We then define the score of each region as the average pixel value subtracted by the standard deviation of the pixel values within the region. Then, we selecte the region with the highest score, and divide it further into four smaller regions. We repeate this process until the size of the selected region is smaller than a pre-specified threshold. For example, in Fig. 2, the red block $I_{\inf}(x,y)$ is finally selected, $I_{\inf}^{\perp}(x,y)$ and $I_{\inf}^{\parallel}(x,y)$ are the fully backscattered areas that correspond to $I_{\inf}(x,y)$. p_A can be obtained by:

$$p_A = mean\left(\frac{A^{\perp}(x,y) - A^{\parallel}(x,y)}{\mathrm{A}^{\perp}(\mathrm{x},\mathrm{y}) + \mathrm{A}^{\parallel}(\mathrm{x},\mathrm{y})}\right) = mean\left(\frac{I_{\inf}^{\perp}(x,y) - I_{\inf}^{\parallel}(x,y)}{I_{\inf}^{\perp}(x,y) + I_{\inf}^{\parallel}(x,y)}\right) \tag{8}$$

Then, A_∞ can be solved by:

$$A_\infty = I_{\inf}(p^*) \tag{9}$$

with

$$p^* = \arg\min_{p \in I_{\inf}} \left\| I_{\inf}^{c}(p) - 255 \right\|, \; c \in \{r,g,b\}$$

where p is the pixel coordinate in the selected region, $I_{\inf}(p)$ is the fully backscatterd area in I, p^* denotes the location of the brightest pixel among those selected region pixels, while r, g, b represented the red, green and blue color elements, respectively. Finally, according to Eqs. (3, 7, 8, 9), the degraded image is reconstructed.

3. EXPERIMENT RESULTS

In order to prove the universality of our method, two groups of experiment are performed. The light source all over the scene is natural illumination, and a rotating linear polarizer is mounted in front of the CCD as the analyzer. Two different material targets in our experiment: paper and metal products, which have some different detail information in their surface. The targets and the CCD camera are put in the water container, meanwhile, pour coffee inside to simulate muddy underwater environment.

3.1 Qualitative Result

Through rotating the analyzer to the parallel and orthogonal polarization state, we obtain the two groups of orthogonal polarization image as shown in Fig. 3 and Fig. 4. The first group of original images are shown in Fig. 3(a), one is the co-linear image $I^{\parallel}(x,y)$ with the value of contrast calculated to be 0.40, and the other is cross-linear image $I^{\perp}(x,y)$ with the value of contrast calculated to be 0.38. As shown in Fig. 3(b), the words on the paper is indistinguishable in the original intensity image, but the word is legible in our restoration image. The value of contrast in our result with simple image processing reaches 0.65, it means that the contrast has nearly doubled compared with cross-linear image. Visually, the quality and details of the image is greatly improved.

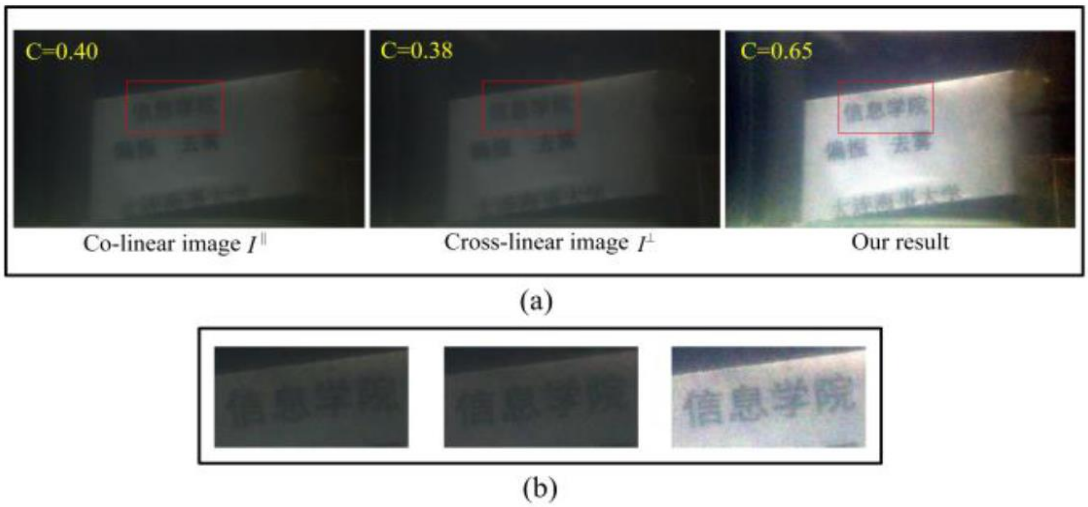

Figure 3. (a) The first group of original polarimetrc images and the enhanced images by the proposed method; (b) the enlarged views of the red rectangles.

The histogram distribution is used for further intuitively illustrate the image improved quality. The red-blue-green curves represent the distribution of the histogram of three color channels, respectively. Fig. 4(a)(b) shows the original orthogonal polarization image in the second experiment and Fig. 4(c) shows the recovered image by our method. The histogram distribution of initial images is mainly concentrated in a narrow scale range, the details of entire image is obscured. The histogram distribution of the enhanced image by the proposed method is wider than before, it indicates a better result of the ehhancement. Fig. 5 shows the comparison with other enhancement methods. In Fig. 5, the first two columns is original orthogonal polarimetric images. The last two columns show the enhanced images by Schechner's method [8] and Fan's method [16]. It can be observed that the enhanced images with improved contrast and satisfactory color is produced by the proposed method.

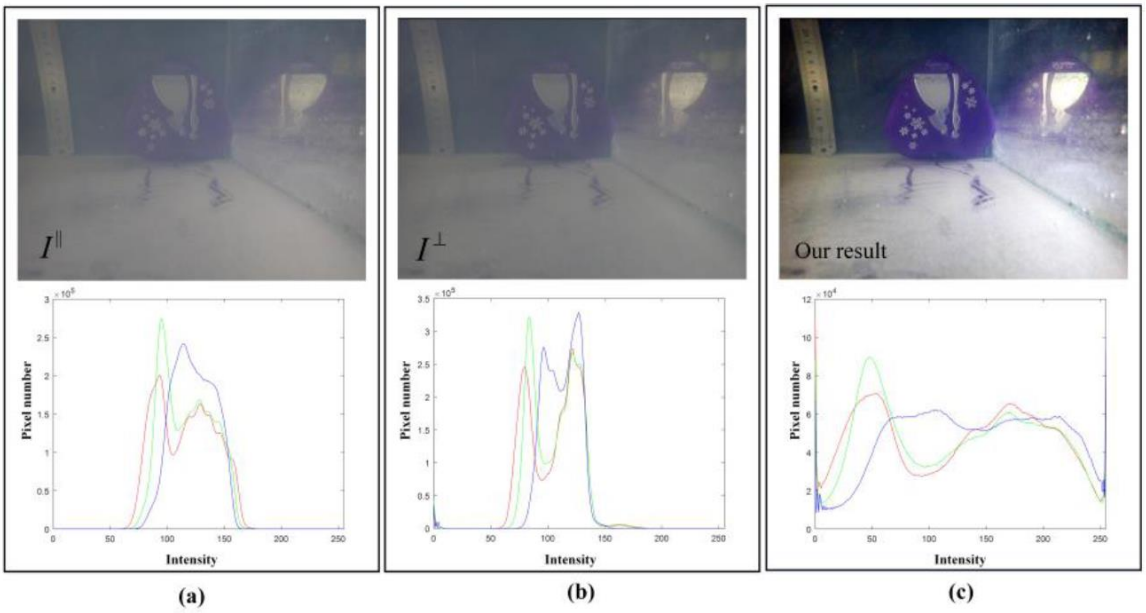

Figure 4. (a), (b) The second group of original orthogonal polarimetric images and their histogram. (c) The enhanced images by the proposed method and its histogram. The red-blue-green curves represent the distribution of the histogram of three color channels, respectively.

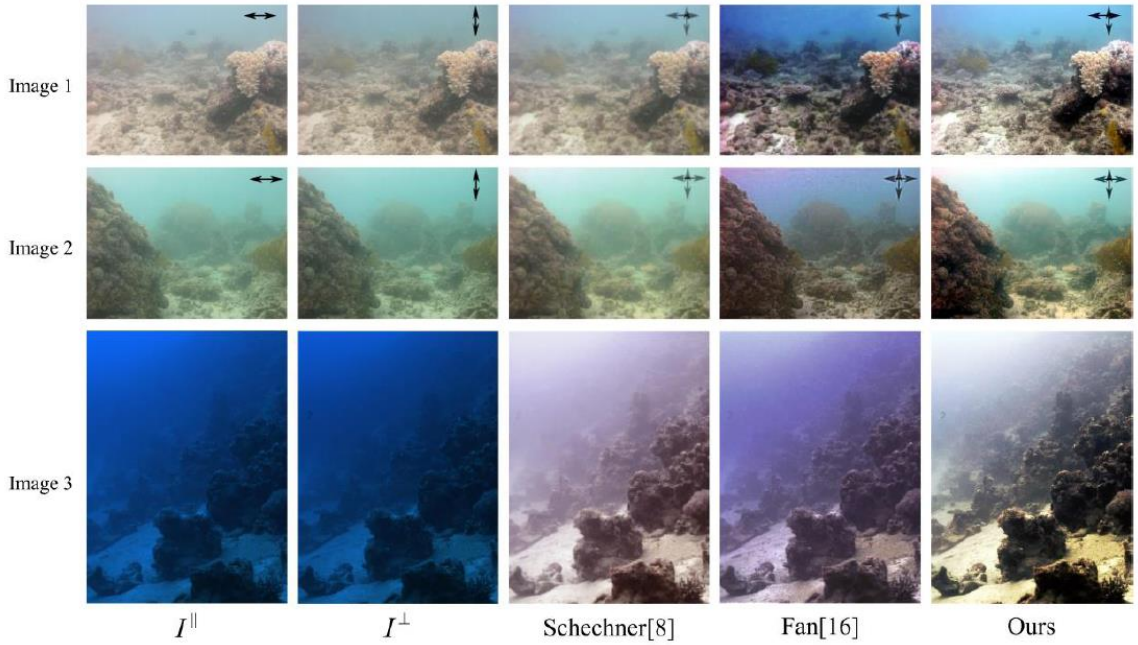

Figure 5. Comparison of underwater image enhancement methods.

3.2 Quantitative Result

Moreover, information entropy (H) and contrast (C) are employed to quantitative evaluate the quality of the images in Fig. 5. Higher value of C and H indicates that the image has higher image contrast and more detail information. The contrast of an image is given by Eq. 10. Li's method [16] is reproduced by us to compare the quality of enhanced images. C and H values of enhanced images are shown in Table 1.

$$C = \sqrt{\frac{\sum_{y=0}^{m-1}\sum_{x=0}^{n-1}\left(g(x,y)-brightness\right)^2}{m\times n}},\ brightness = \frac{\sum_{y=0}^{m-1}\sum_{x=0}^{n-1} g(x,y)}{m\times n} \tag{10}$$

where $g(x,y)$ is the enhanced image, $brightness$ is the mean intensity of the image.

Table 1. The values of quantitative comparison.

Image	Method	C	H
Image1	Li	0.14	5.99
	Our	**0.37**	**7.56**
Image2	Li	0.16	6.70
	Our	**0.49**	**7.91**
Image3	Li	0.26	7.14
	Our	**0.57**	**7.93**

4. CONCLUSION

In this paper, we proposed an underwater adaptive polarimetric image recovery model with considering the differences in light attenuation between in atmosphere and in water. Then, we applied quad-tree decomposition to extract the fully back-scatter area to estimate these parameters of the novel model automatically. Our algorithm is effective and even works in turbid waters, we will apply it to the real-time image processing for underwater robot in the future.

ACKNOWLEDGMENT

This work was supported in part by the National Natural Science Foundation of China Grant 61802043 and Grant 61370142, by the Fundamental Research Funds for the Central Universities Grant 3132016352 and Grant 3132018195.

REFERENCES

[1] Y.G. Li, H.M. Lu, L.F. Zhang, J.R. Li and S. Serikawa, "Real-time visualization system for deep-sea surveying," Mathematical Problems in Engineering (2014).

[2] X.D. Tang, W. Zhu, Y.J. Pang and Y. Li, "Target recognition system based on optical vision for AUV," Robot 312, 171-178, (2009).

[3] W.J. Zeng, Y.R Xu, L. Wan and T.D. Zhang, "Robotics Vision-Based System of Autonomous Underwater Vehicle for an Underwater Pipeline Tracker," Shanghai Jiaotong Univ.(Sci.) 02, 178-183+189, (2012).

[4] C. Spampinato, S. Palazzo and B. Boom, "Understanding fish behavior during typhoon events in real-life underwater environments," Multimedia Tools and Applications 1-38, (2012).

[5] A. K. Jain. Fundamentals of Digital Image Processing, Prentice Hall, (1989).

[6] C.Y. Li, J.C. Guo, R.M. Cong, Y. W. Pang and B. Wang, "Underwater image enhancement by dehazing with minimum information loss and histogram distribution prior," IEEE Transactions on Image Processing, **2512**, 5664-5677, (2016).

[7] Y.Y. Schechner, S.G. Narasimhan, and S.K. Shree, "Polarization-based vision through haze," Applied optics **423**, 511-525, (2003).

[8] Y.Y. Schechner, and N Karpel, "Recovery of underwater visibility and structure by polarization analysis," IEEE Journal of oceanic engineering **303**, 570-587, (2005).

[9] J. Fade, S. Panigrahi, A. Carré,"Long-range polarimetric imaging through fog,"Appl. Opt. 53, 3854-3865, (2014).

[10] S. Panigrahi, J. Fade and M. Alouini, "Adaptive polarimetric image representation for contrast optimization of a polarized beacon through fog," Opt. **17**, 065703, (2015).

[11] J. Liang, L.Y. Ren, E.S. Qu, B.L. Hu and Y.L. Wang, "Method for enhancing visibility of hazy images based on polarimetric imaging," Photon. Res. **2**, 38-44, (2014).

[12] Y. Qu and Z. Zou, "Non-sky polarization-based dehazing algorithm for non-specular objects using polarization diference and global scene feature," Opt. Express **25**, 25004 – 25022, (2017).

[13] J. Liang, L.Y. Ren, H.J. Ju, W.F. Zhang and E.S. Qu, "Polarimetric dehazing method for dense haze removal based on distribution analysis of angle of polarization," Opt. Express **23**, 26146-26157, (2015).

[14] X.B. Li, H.F. Hu, L. Zhao, "Polarimetric image recovery method combining histogram stretching for underwater imaging," Scientific Reports **8**, (2018).

[15] J.H. Kim, W.D. Jang, J.Y. Sim and C.S. Kim, "Optimized contrast enhancement for real-time image and video dehazing," Journal of Visual Communication & Image Representation **243**, 410-425, (2013).

[16] X.N. Fan, J.Y. Chen, X.W. Zhang, P.F. Shi, Z. Zhang, "Underwater polarized images restoration algorithm based on structural similarity," Journal of Image and Graphics **237**, 1033-1041, (2018).